Contents lists available at ScienceDirect

Journal of Reproductive Immunology

journal homepage: www.elsevier.com/locate/jri

The expression of TIM-3 and Gal-9 on macrophages and Hofbauer cells in the placenta of preeclampsia patients

Johanna Mittelberger [a], Marina Seefried [a], Sanja Löb [b], Christina Kuhn [a], Manuela Franitza [a], Fabian Garrido [a], Nina Ditsch [a], Udo Jeschke [a,*], Christian Dannecker [a]

[a] Department of Obstetrics and Gynecology, University Hospital Augsburg, Stenglinstraße 2, Augsburg 86156, Germany
[b] Department of Obstetrics and Gynecology, University Hospital, University of Wuerzburg, Josef-Schneider-Str. 4, Würzburg 97080, Germany

A B S T R A C T

Preeclampsia is a disorder of pregnancy characterized by endothelial dysfunction, abnormal placentation, systemic inflammation, and altered immune reaction. The aim of this study was to investigate the immune checkpoint molecules TIM-3 and Gal-9 on macrophages and Hofbauer cells (HBC) in the placenta of preeclampsia patients. Immunohistochemistry and Immunofluorescence was used to characterize the expression of the macrophage markers CD68 and CD163, CK7 and the proteins TIM-3 and Gal-9 in the placentas of preeclampsia patients comparing it to the placentas of healthy pregnancies. Double immunofluorescence staining (TIM-3 with CD3/CD19/CD56) was used to analyze the TIM-3 expression on other immune cells (T cells, B cells, NK cells) within the chorionic villi. The expression of TIM-3 on decidual macrophages did not significantly differ between the preeclamptic and the control group (p = 0.487). When looking at the different offspring we saw an upregulation of TIM-3 expression on decidual macrophages in preeclamptic placentas with female offspring (p = 0.049). On Hofbauer cells within the chorionic villi, the TIM-3 expression was significantly downregulated in preeclamptic cases without a sex-specific difference (p < 0.001). Looking at the protein Gal-9 the expression was proven to be downregulated both, on decidual macrophages (p = 0.003) and on Hofbauer cells (p = 0.002) within preeclamptic placentas compared to healthy controls. This was only significant in male offspring (p < 0.001 and p = 0.013) but not in female offspring (p = 0.360 and p = 0.068). While TIM-3 expression within the extravillious trophoblast and the syncytiotrophoblast was significantly downregulated (p < 0.001 and p = 0.012) in preeclampsia, the expression of Gal-9 was upregulated in (p < 0.001 and p < 0.001) compared to healthy controls. The local variations of the immune checkpoint molecules TIM-3 and Gal-9 in the placenta may contribute to the inflammation observed in preeclamptic patients. It could therefore contribute to the pathogenesis and be an important target in the treatment of preeclampsia.

1. Introduction

Preeclampsia is a pregnancy-specific disease and one of the most serious complications in pregnant women. It is defined as a new-onset gestational hypertension after the 20th week of pregnancy associated with proteinuria and/or other organ dysfunctions. Affecting 5–7 % of all pregnancies worldwide, it is the leading cause of fetal and maternal morbidity and mortality (Rana et al., 2019). Two types of preeclampsia are distinguished in the literature: early- and late-onset preeclampsia. While early-onset is defined by occurring before the 34th week of pregnancy, late-onset preeclampsia arises after the 34th week (Tranquilli et al., 2013; Valensise et al., 2008). There is no causal treatment

except for delivery which often ends in premature birth with its possible complications for the fetus. The importance and significance of this condition is also highlighted by possible effects in later life. Studies showed that women with preeclampsia during pregnancy have an increased risk of developing cardiovascular disease such as hypertension or ischemic heart disease later in life (Rana et al., 2019; Sukmanee and Liabsuetrakul, 2022; Vest and Cho, 2012; Xu et al., 2022). The exact pathogenesis of preeclampsia, which has been shown to be multifactorial, is still not fully understood and the subject of ongoing research. Abnormal placentation with a defective trophoblast invasion and an increase of anti-angiogenic factors appear to play a central role in etiology (Rambaldi et al., 2019; Yeh et al., 2013).

Because the semi-allogenic fetus must be accepted by the mother during the whole gestational period, pregnancy poses a major challenge to the maternal immune system (Ander et al., 2019). By maintaining immunological tolerance between mother and child, the decidua therefore plays an important role locally in the placenta. This part of the placenta has been shown to become a focus of inflammation in pre-eclampsia, which is involved in the etiology of the disease (Vishnyakova et al., 2021). Proinflammation is also evident systemically in preeclampsia. Regulatory T-cells and anti-inflammatory cytokines, for example, were shown to be reduced in preeclampsia, while pro-inflammatory cytokines and CD4(+) T-cells were increased (Aggarwal et al., 2019; Harmon et al., 2016).

This proinflammation can also be influenced by macrophages, an important cell line in local immunity and one of the largest cell populations at the maternal-fetal-interface. Depending on their polarization, they can have pro-inflammatory (M1 macrophages) or anti-inflammatory (M2 macrophages) functions. While in normal pregnancy the macrophages are mostly M2-polarized (Yao et al., 2019), different studies showed an increase of M1-macrophages and a decrease of M2-macrophages in PE-placentas, leading to proinflammation (Tang et al., 2013; Yang et al., 2017; Yao et al., 2019). Data about the total number of macrophages in the PE-placenta are conflicting with some studies showing an increase (Huang et al., 2010; Li et al., 2016; Reister et al., 2001) and others showing a decrease (Bürk et al., 2001; Williams et al., 2009) in the quantity of macrophages. Not only the maternal macrophages but also the fetal macrophages within the chorionic villi, the Hofbauer cells, were proven to be downregulated in preeclampsia (Reyes and Golos, 2018).

Another important effector in immunological homeostasis and maternal-fetal-tolerance are immune checkpoint molecules such as the T-cell immunoglobulin and mucin domain-containing protein 3 (TIM-3) and its ligand Galectin-9 (Gal-9). When activated by their ligand, they mostly have an inhibitory effect on the immune system by negatively regulating effector cells such as T cells. Thereby these molecules are involved in immune regulation during tumor growth, autoimmunity and infections (Kandel et al., 2021). In addition, these immune checkpoint molecules are crucial for reproductive immunology and maintaining the pregnancy (Mittelberger et al., 2022; Mohamed Khosroshahi et al., 2021). Data suggests that there are multiple variations of the molecules in pregnancy complications such as preeclampsia. While most of the studies focus on peripheral blood, little is known about TIM-3 and Gal-9 within the placenta and the maternal-fetal-interface (Mittelberger et al., 2022).

In a previous study we investigated the differences in the number of macrophages and the expression of PD1/PD-L1, another important immune checkpoint system, in the preeclamptic placenta. This was done with the same patient cohort than the present study. We found a significant downregulation of the two macrophage markers CD68 and CD163 on maternal macrophages and Hofbauer cells in the preeclamptic group. Also PD1 and PD-L1 were downregulated on placental macrophages in preeclampsia which could have a potential influence in the pathogenesis of the disease by promoting proinflammation (Mittelberger et al., 2023).

Based on our previous investigation, this study aims to verify possible changes in the expression of TIM-3 and Gal-9 on macrophages within the placenta in preeclampsia and their possible role in the pathogenesis of the disease.

2. Materials and methods

2.1. Study subjects

The Ethics Committee of Ludwig Maximilian University (LMU) in Munich, Germany, approved the study in July 2021. After written informed consent, the placental tissue from 40 preeclampsia patients (20 female offspring, 20 male offspring) who gave birth at University

Hospital Augsburg in 2016–2020 by cesarean section was obtained and retrospectively included into the study. The preeclampsia patients had to be at least 30+0 weeks of gestation and fulfill the diagnostic criteria for preeclampsia in order to be eligible for inclusion. Patients who simultaneously had a HELLP-syndrome (hemolysis, elevated live enzymes, and low platelet count) or a fetal growth restriction (FGR) were also suitable for inclusion.

In order to form a control group, we obtained placental tissue from 40 healthy patients (20 female offspring, 20 male offspring) who had delivered in 2018–2021 by cesarean section. They were also retrospectively enrolled in the study after written informed consent. The two groups were matched by gestational week at delivery, fetal sex, and maternal age +/- 5 years. To exclude confounding factors, we defined the following exclusion criteria for the healthy control group: fetal growth restriction, gestational diabetes, obesity with a BMI $> 30 \text{ kg/m}^2$, multiple pregnancy, fertility treatment, signs of systemic inflammation in the blood, placental disorders such as placenta accreta/percreta/increta.

After buffering in 4 % formalin immediately after delivery, the placentas were dissected out of their central part at the institute for Pathology, Augsburg University Hospital, containing decidua, extravillious and villious trophoblast. The samples were then embedded in paraffin

Table 1
Clinical details of the study population separated by time of onset.

	Preeclampsia (n=40)		Control (n=40)	p-value
	Early onset (n = 18)	Late onset (n = 22)		
Maternal age at delivery, years	32.18 ± 4.96		32.57 ± 4.91	p = 0.718
	32.33 ± 4.19	32.05 ± 5.61	-	p = 0.858
BMI	29.34 ± 7.12		23.54 ± 3.31	**p < 0.001**
	30.42 ± 7.89	28.46 ± 6.47	-	p = 0.393
Gravidity	1.40 ± 0.73		2.03 ± 1.03	**p = 0.001**
	1.44 ± 0.78	1.36 ± 0.73	-	p = 0.798
Parity	1.30 ± 0.65		1.68 ± 0.80	**p = 0.007**
	1.33 ± 0.69	1.27 ± 0.63	-	p = 0.840
Gestational age at delivery	35.00 ± 2.06		35.00 ± 2.18	p = 0.957
	33.22 ± 1.48	36.45 ± 1.10	-	**p < 0.001**
Fetal birthweight, g	2089.73 ± 594.66		2362.50 ± 538.03	**p = 0.021**
	1677.44 ± 417.34	2427.05 ± 500.83	-	**p < 0.001**
Birth percentile	24.67 ± 23.22		45.68 ± 22.05	**p < 0.001**
	26.11 ± 20.93	23.43 ± 25.46	-	p = 0.426
APGAR 10 min	9.55 ± 0.60		9.53 ± 0.68	p = 0.973
	9.67 ± 0.49	9.45 ± 0.67	-	p = 0.427
Umbilical artery pH	7.26 ± 0.07		7.29 ± 0.09	**p < 0.001**
	7.26 ± 0.04	7.25 ± 0.09	-	p = 0.370
Placental weight	384.70 ± 125.10		460.13 ± 122.89	**p = 0.005**
	308.56 ± 79.11	447.00 ± 122.32	-	**p < 0.001**
HELLP-Syndrome	n = 9		n = 0	-
Fetal growth restriction	n = 5		n = 0	-

and cut into 2–3μm thick slices using a sliding microtome.

Table 1 (separated by time of onset) and Table 2 (separated by fetal sex) show the clinical details of the study population.

For all significantly different clinical characteristics we performed confounder analysis by linear regression model. Results can be seen in the supplementary table 1.

Table 2
Clinical details of the study population separated by fetal sex.

	Preeclampsia (n = 40) Preeclampsia female (n = 20) Preeclampsia male (n = 20)	Control (n = 40) Control female (n = 20) Control male (n = 20)	p-value
Maternal age at delivery, years	32.18 ± 4.96	32.57 ± 4.91	p = 0.718
	31.65 ± 4.84	31.45 ± 4.15	p = 0.889
	32.70 ± 5.15	33.70 ± 5.44	p = 0.554
BMI	29.34 ± 7.12	23.54 ± 3.31	**p < 0.001**
	31.56 ± 8.69	24.00 ± 3.18	**p < 0.001**
	27.10 ± 4.24	23.08 ± 3.46	**p = 0.002**
Gravidity	1.40 ± 0.73	2.03 ± 1.03	**p = 0.001**
	1.40 ± 0.75	2.10 ± 1.17	**p = 0.035**
	1.40 ± 0.75	1.95 ± 0.89	**p = 0.043**
Parity	1.30 ± 0.65	1.68 ± 0.80	**p = 0.007**
	1.30 ± 0.66	1.80 ± 0.83	**p = 0.043**
	1.30 ± 0.66	1.55 ± 0.76	p = 0.221
Gestational age at delivery	35.00 ± 2.06	35.00 ± 2.18	p = 0.957
	34.95 ± 2.06	35.10 ± 2.20	p = 0.825
	35.05 ± 2.11	34.90 ± 2.22	p = 0.828
Birthweight, g	2089.73 ± 594.66	2362.50 ± 538.03	**p = 0.021**
	2002.80 ± 526.17	2371.05 ± 570.56	**p = 0.040**
	2176.65 ± 658.10	2353.95 ± 518.15	p = 0.350
Birth percentile	24.67 ± 23.22	45.68 ± 22.05	**p < 0.001**
	23.84 ± 22.93	48.70 ± 20.18	**p < 0.001**
	25.45 ± 24.06	42.65 ± 23.91	**p = 0.010**
APGAR 10 min	9.55 ± 0.60	9.53 ± 0.68	p = 0.973
	9.60 ± 0.50	9.60 ± 0.75	p = 0.640
	9.50 ± 0.69	9.45 ± 0.61	p = 0.718
Umbilical artery pH	7.26 ± 0.07	7.29 ± 0.09	**p < 0.001**
	7.26 ± 0.07	7.29 ± 0.10	**p = 0.006**
	7.25 ± 0.07	7.29 ± 0.07	**p = 0.038**
Placental weight	384.70 ± 125.10	460.13 ± 122.89	**p = 0.005**
	380.75 ± 115.95	462.75 ± 109.74	**p = 0.027**
	388.65 ± 136.55	457.50 ± 137.62	p = 0.121

2.2. Immunohistochemistry

For immunohistochemistry, paraffin sections were deparaffinized with Roticlear® and immersed in 100 % ethanol. To block endogenous peroxidase activity, the samples were incubated in 3 % (for CD68, CD163, Gal-9) / 6 % (for TIM-3) H_2O_2 in methanol for 20 min and then rehydrated in a gradient going from alcohol to distilled water. Next, the sections were placed in a high-pressure pot with boiling sodium citrate buffer pH 6.0 (for CD68, CD163 and Gal-9) and Tris EDTA buffer pH 9.0 (for TIM-3) for antigen recovery for 6 min.

The slices were washed in distilled aqua and phosphate-buffered saline (PBS). Next, they were treated with a blocking solution (Reagent 1; ZytoChem Plus HRP Polymer System IgG kit (Mouse/Rabbit) from Zytomed) for 5 min to saturate the electrostatic charges. Subsequently, the slices were incubated with the respective primary antibody (against CD68, CD163, TIM-3, Gal-9) for 16 hours at 4°C. After the slides were washed with PBS, the bound primary antibodies were visualized using the ZytoChem Plus HRP Polymer System IgG kit (Mouse/Rabbit), (Zytomed, Berlin, Germany) and the liquid DAB+ Substrate Chromogen System (Agilent Technologies, Santa Clara, USA). Counterstaining of the slides was done using Mayer's acid hemalum for 2 min and stained blue in tap water for 5 min. The samples were then dehydrated in an ascending alcohol series, treated with Roticlear® and coated with RotiMount (Carl Roth, Germany). All antibodies used in this study are listed in Table 3.

To determine the number of antigen-presenting macrophages and Hofbauer cells, the number of positive cells in three sections was counted using a 40x lens. The counted number of these three sections were then summed. Remmele's semi-quantitative immunoreactive score (IRS) was used to assess the intensity and distribution patterns of TIM-3 and Gal-9 antigen expression within the extravillious trophoblast and syncytiotrophoblast. The IRS is calculated by multiplying the intensity level of the optical staining (0=none, 1=weak, 2=moderate and 3=strong staining) and the percentage of cells with positive staining (also divided into 4 categories: 0=no staining, 1= <10 % of cells, 2=10–50 % of cells, 3=51–80 % of cells and 4=more than 80 % of cells).

The intensity, distribution pattern, and counting of the immuno-chemical staining reactions were assessed by two independent observers who were blinded; in twelve cases (n = 15 %) the two observers' assessments differed. These cases were reevaluated jointly by both observers. After reevaluation, both observers reached the same conclusion. The agreement before the reevaluation was 85 %.

In order to proof that the immunohistochemical staining in Figs. 1 and 2 really show decidual side and not parts like the stem villi, we performed immunohistochemical staining for the decidual marker IGFBP1. The results as well as the staining protocol can be seen in the

Table 3
List of the used primary antibodies.

| Antibody	Isotype	Clone	Dilution	Source
Anti-CD68	Rabbit IgG	Monoclonal; clone D4B9C	1:1000	Cell Signaling, USA
Anti-CD163	Mouse IgG1	Monoclonal; clone OTI2G12	1:2000	Abcam, UK
Anti-TIM-3	Rabbit IgG	Monoclonal; clone D5D5R	1:150 or 1:75	Cell Signaling, USA
Anti-Gal-9	Mouse IgG$_{2B}$	Monoclonal; clone 1005401	1:300	Cell Signaling, USA
Anti-CK7	Mouse IgG1	Monoclonal; clone OV-TL12/30	1:200	Agilent, USA
Anti-CD3	Rabbit IgG	Monoclonal; clone 2GV66	Ready-to-use	Roche, Switzerland
Anti-CD19	Rabbit IgG	Monoclonal; clone D4V4B	1:1000	Cell Signaling, USA
Anti-CD56	Rabbit IgG	Monoclonal; clone E7X9M	1:100	Cell Signaling, USA
Anti-IGFBP1	Mouse IgG	Monoclonal; clone H-5	1:800	Santa Cruz Biotechnology, USA
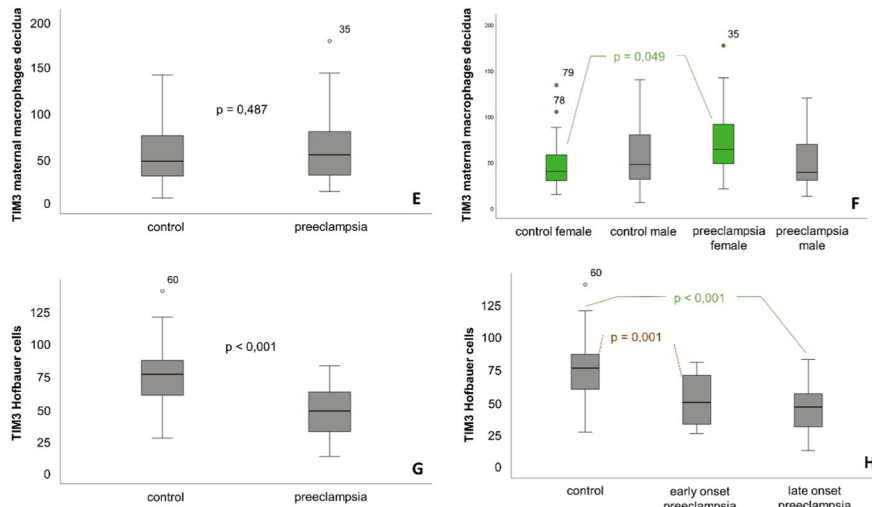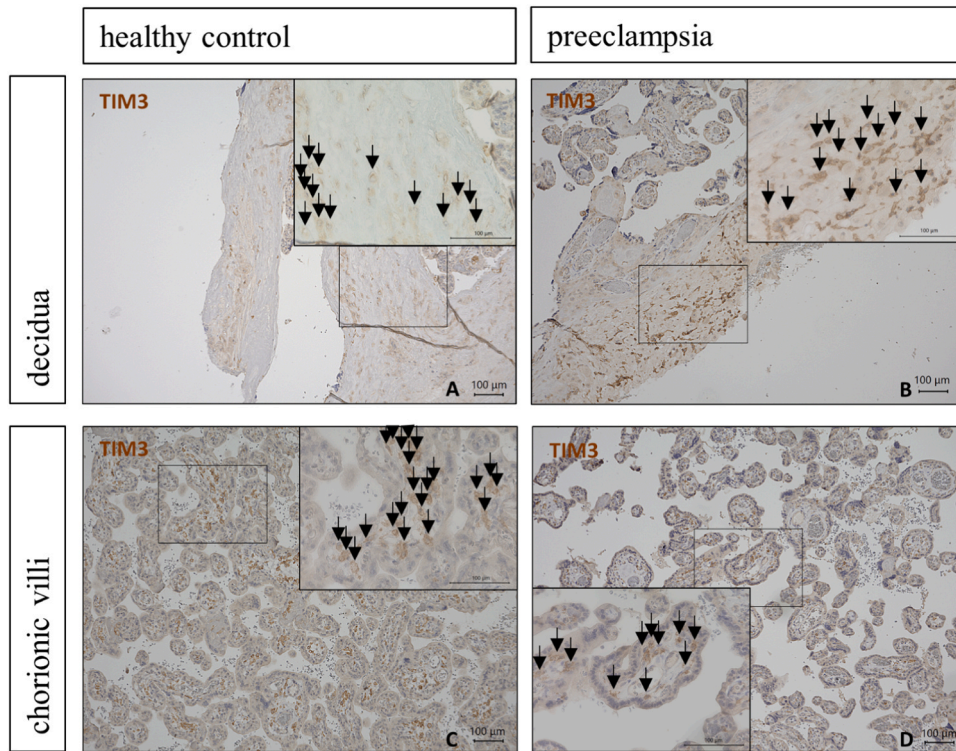
Fig. 1. Representative slides of immunohistochemical staining for TIM-3 expression in the decidua of a healthy control (A) and a preeclampsia patient (B) as well as the chorionic villi of a healthy control (C) and a preeclampsia patient (D). Pictures were taken with a 10x lens. The inserts represent a magnification with a 40x lens. The black frame shows where the magnified inserts are taken from. The arrows point to the TIM-3-positive macrophages in parts (A) and (B)and HBCs in parts (C) and (D). Scale bars are 100 μm. Boxplot E shows the difference in TIM-3 expression on maternal macrophages with an upregulation in female preeclamptic offspring seen in boxplot F. The significant downregulation of TIM-3 on Hofbauer cells in preeclampsia is illustrated in boxplots G and H. The boxplots represent the number of positive cells within the immunohistochemical staining.

supplementary.

2.3. Triple immunofluorescence

Triple immunofluorescence staining enables simultaneously characterizing specific antigens on the same cell. For deparaffinization, the same samples fixed in formalin and embedded in paraffin were placed in Roticlear® for 20 min. The sections were then passaged in ethanol in descending order of concentration (100 %, 70 %, 50 %) and washed with distilled water. Antigen unmasking was performed by heat pretreatment using a pressure cooker with EDTA buffer pH 9.0 (for TIM-3) or sodium citrate buffer pH 6,0 (for Gal-9). After washing in distilled water and PBS for 4 min, the slices were incubated with immunofluorescence blocking buffer (Cell Signaling; No. 12411 S) to prevent non-specific staining. The solution was removed after 60 min, and the primary antibodies were applied. CD68 (1:3000) and CD163 (1:4000) were stained together in dilution medium (Agilent; No. S302281–2) to differentiate the cells in a double staining method. The slices were then incubated at 4 °C for 16 hours. After washing in PBS and darkening the experimental chamber, the mixed secondary antibodies were applied:
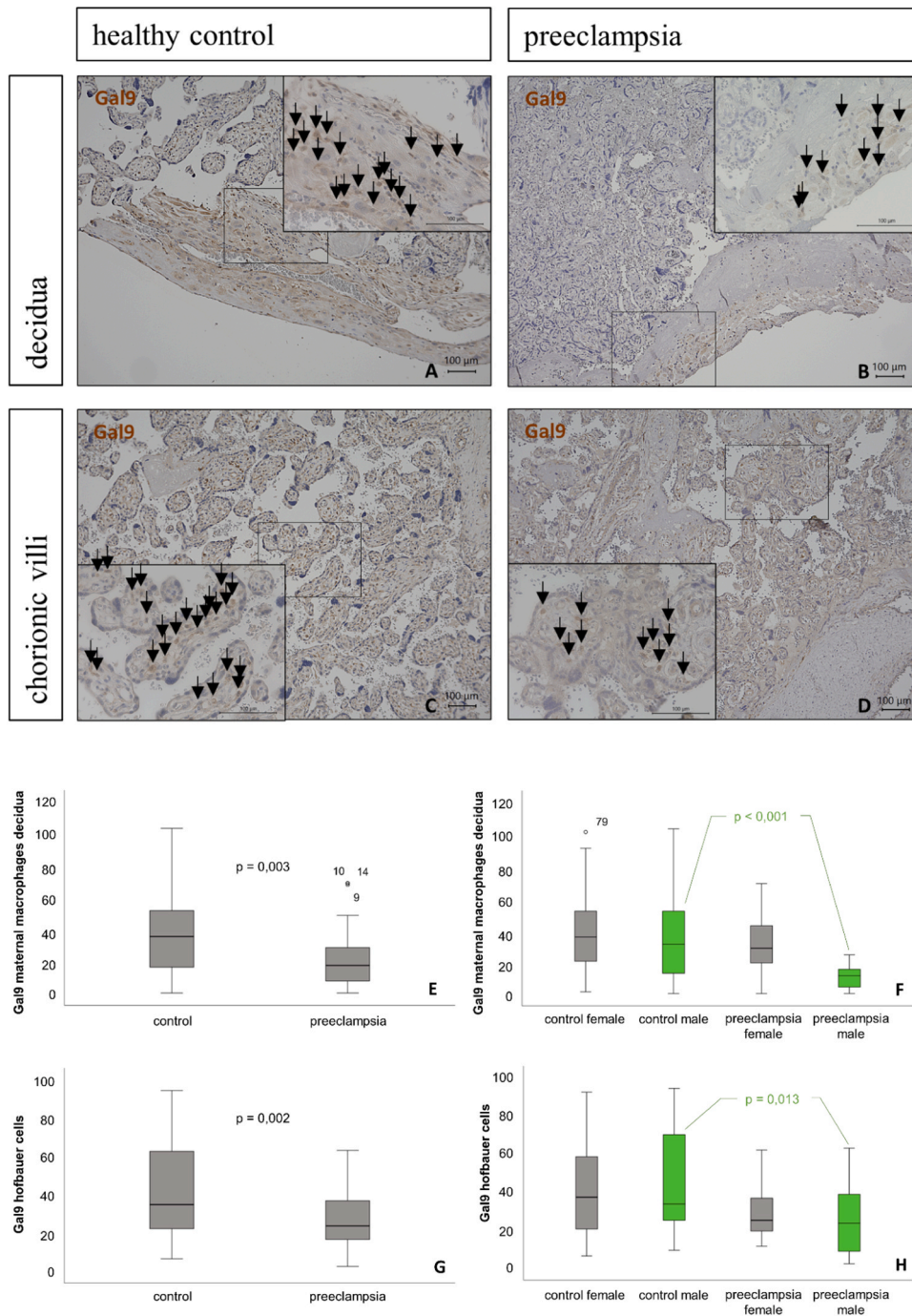
Fig. 2. Representative slides of immunohistochemical staining for Gal-9 expression in the decidua of a healthy control (A) and a preeclampsia patient (B) as well as the chorionic villi of a healthy control (C) and a preeclampsia patient (D). Pictures were taken with a 10x lens. The inserts represent a magnification with a 40x lens. The black frame shows where the magnified inserts are taken from. The arrows point to the Gal-9-positive macrophages in parts (A) and (B) and HBCs in parts (C) and (D). Scale bars are 100 μm. Boxplot E shows the downregulation of Gal-9 on maternal macrophages with a sex-specific difference seen in Boxplot F. The significant downregulation of Gal-9 on Hofbauer cells in preeclampsia is illustrated in boxplots G and H. The boxplots represent the number of positive cells within the immunohistochemical staining.

goat anti-mouse IgG antibody conjugated with Cy-5 at a ratio of 1:100 (Dianova, Hamburg, Germany, 115–175–166) for purple staining and goat anti-rabbit IgG antibody conjugated with Cy-3 at a ratio of 1:500 (Dianova, Hamburg, Germany, 111–165–144) for red staining. After incubation for 30 min, PBS was used to wash off excess secondary antibodies. At this point, samples were blocked with Fab Fragment Donkey Anti-goat IgG antibody (Dianova, Hamburg, Germany, 705–007–003) at a ratio of 1:50 in dilution medium (Agilent; No. S302281–2) for 30 min in the dark and then washed in PBS for 4 min. In the next step, the third

primary antibody Gal-9 at a ratio of 1:300 in dilution medium (Agilent; No. S302281–2) or TIM-3 at a ratio of 1:150 in dilution medium (Agilent; No. S302281–2) was applied and incubated at 4 °C overnight. After washing in PBS, an anti-rabbit IgG secondary antibody conjugated with Alexa Fluor 488 (Thermo Fisher, Massachusetts, USW, No. A-11008) was applied at a ratio of 1:500 in dilution medium (Agilent; No. S302281–2) and incubated for 30 min at room temperature in the dark, resulting in green staining. The slices were washed again in PBS for 4 min and covered with TrueBlack at a ratio of 1:20 in 70 % ethanol for

1 minute in the dark. After washing them again in PBS for 4 min, they were dried at room temperature in the dark and covered with DAPI fluorescent mounting medium, which stains the nuclei blue.

The triple staining was assessed and evaluated with a fluorescence microscope (Keyence, Osaka, Japan).

2.4. Double immunofluorescence

Double immunofluorescence staining enables simultaneously characterizing two antigens on the same cell. This method was used for TIM-3 and Gal-9 together with CK7 (marker for extravillious trophoblast cells) as wells as TIM-3 together with CD3 (marker for T cells), CD19 (marker for B cells) and CD56 (marker for NK cells). The detailed staining protocols are listed in the supplementary.

2.5. Statistical analysis

SPSS version 28 was used for the statistical analysis. The data was first tested for normal distribution by calculating the Kolmogorov-Smirnov test. The t-test was used to compare mean values for data with normal distribution. For data not normally distributed, the Mann-Whitney U signed rank test was calculated for comparing the means. Those calculations were illustrated by boxplots, where the boxes represent the range between the 25th and 75th percentiles and the horizontal represents the median. The 5th and 95th percentiles are displayed by the bars and the outliers by dots. Confounding analysis was performed using a linear regression path for BMI and other clinical data. This was performed to rule out an effect of clinical data on macrophages/checkpoint molecules. Results with p-values < 0.05 were considered significant.

3. Results

3.1. Variations of TIM-3 expression in preeclampsia

The number of TIM-3-positive Hofbauer cells was shown to be significantly downregulated in the placenta of preeclamptic patients compared to healthy controls ($p < 0.001$). It was evident in both, early-onset and late-onset preeclampsia without a sex-specific difference. This is illustrated in Fig. 1, parts C/D/G/H.

The expression of TIM-3 on maternal macrophages within the decidua did not significantly differ between the preeclamptic and the control group ($p = 0.487$). However, comparing the different sexes, TIM-3 showed a significant upregulation on maternal macrophages in female preeclamptic cases ($p = 0.049$) while this was not evident in male preeclamptic cases ($p = 0.285$). This is seen in Fig. 1, parts A/B/E/F.

The immunoreactive score of TIM-3 expression on extravillious trophoblasts was lower in preeclampsia compared to control cases ($p < 0.001$). Within the syncytiotrophoblast the TIM-3 expression was also significantly downregulated in preeclampsia ($p = 0.012$), which was more evident in male offspring ($p = 0.012$) compared to female offspring ($p = 0.324$) and in early-onset ($p = 0.002$) compared to late-onset preeclampsia ($p = 0.249$).

3.2. Downregulation of Gal-9 on maternal macrophages and Hofbauer cells in preeclampsia

The expression of Gal-9 on maternal macrophages within the decidua was shown to be significantly downregulated in preeclamptic cases compared to controls ($p = 0.003$), as illustrated in Fig. 2, parts A/B/E. This was evident in both, early-onset ($p = 0.018$) and late-onset preeclampsia ($p = 0.030$). Comparing the different sexes showed that the downregulation was only significant in male offspring ($p < 0.001$) but not in female offspring ($p = 0.360$). This can be seen in the boxplot F in Fig. 2.

On Hofbauer cells, immunohistochemistry showed a significant

downregulation of Gal-9-expression in preeclampsia cases compared to controls ($p = 0.002$), which was more evident in male offspring ($p = 0.013$) than in female offspring ($p = 0.068$). This is shown in Fig. 2, parts C/D/G/H. Distinguishing between the onset of preeclampsia showed that the downregulation of Gal-9 on Hofbauer cells was only significant in early-onset ($p = 0.006$) and not in late-onset preeclampsia ($p = 0.133$).

Within the extravillious trophoblast and the syncytiotrophoblast, Gal-9-expression was upregulated in preeclamptic cases compared to controls ($p < 0.001$ and $p < 0.001$).

3.3. Triple Immunofluorescence Staining of TIM-3 and Gal-9 with CD68 and CD163

In order to prove the presentation of the immune checkpoint molecules on decidual macrophages and Hofbauer cells, we performed triple immunofluorescence staining. Thereby the expression of three antigens (CD68, CD163 and either TIM-3 or Gal-9) within the same cell could be demonstrated.

In the following, Fig. 3 shows the immunofluorescence staining of TIM-3 together with CD68 and CD163 within the chorionic villi. Parts A-D represent a control placenta, parts E-H a preeclamptic placenta. The downregulation of TIM-3 on Hofbauer cells within the chorionic villi can be seen in parts C and G by the arrow marked cells. The yellow-orange color in parts D and H represents the expression of all three antigens within the same cell.

Fig. 4 shows the expression of Gal-9 on decidual macrophages within the decidua in a control placenta (parts A-D) and a preeclamptic placenta (parts E-H). The downregulation of Gal-9 is demonstrated by the arrow-marked cells in parts C and G. The yellow-orange color in parts D and H again demonstrates the expression of all three antigens within one cell.

3.4. Double immunofluorescence staining of TIM-3 and Gal-9 with CK7

Double immunofluorescence staining of Cytokeratin 7 together with TIM-3 and Gal-9 was performed to prove the presentation of the immune checkpoint molecules on trophoblast cells.

Fig. 5 shows the immunofluorescence staining of TIM-3 together with CK7 within the decidua. Red color represents TIM-3, green represents CK7 and blue represents the nuclei. The TIM-3 expression is shown in parts A (control placenta) and B (preeclamptic placenta) and the CK7 expression in parts C (control placenta) and D (preeclamptic placenta). A simultaneous presentation of TIM-3 and CK7 was evident both, in the control placenta and in the preeclamptic placenta, which proves the expression of TIM-3 on extravillious trophoblasts. The double staining in the preeclamptic placenta was weaker, which can probably be explained by the downregulation of the immune checkpoint TIM-3 on extravillious trophoblast cells in preeclampsia compared to controls like already suggested in the immunohistochemical staining. Part E demonstrates the double staining of both markers within the chorionic villi of a control placenta which shows that the TIM-3 positive cells are all located inside the villi. The triple staining with macrophage markers (see chapter 3.3) proves that these cells are Hofbauer cells. Within the syncyctiotrophoblast cells no double staining of CK7 and TIM-3 was seen.

Fig. 6 shows the immunofluorescence staining of Gal-9 together with CK7 within the decidua. Red color represents Gal-9, green represents CK7 and blue represents the nuclei. The Gal-9 expression is shown in parts A (control placenta) and B (preeclamptic placenta). Parts C (control placenta) and D (preeclamptic placenta) show the double staining with CK7 which can be seen in both groups. The upregulation of Gal-9-positive extravillious trophoblast cells in the preeclamptic group can clearly be seen within this immunofluorescence staining, marked by the arrows.
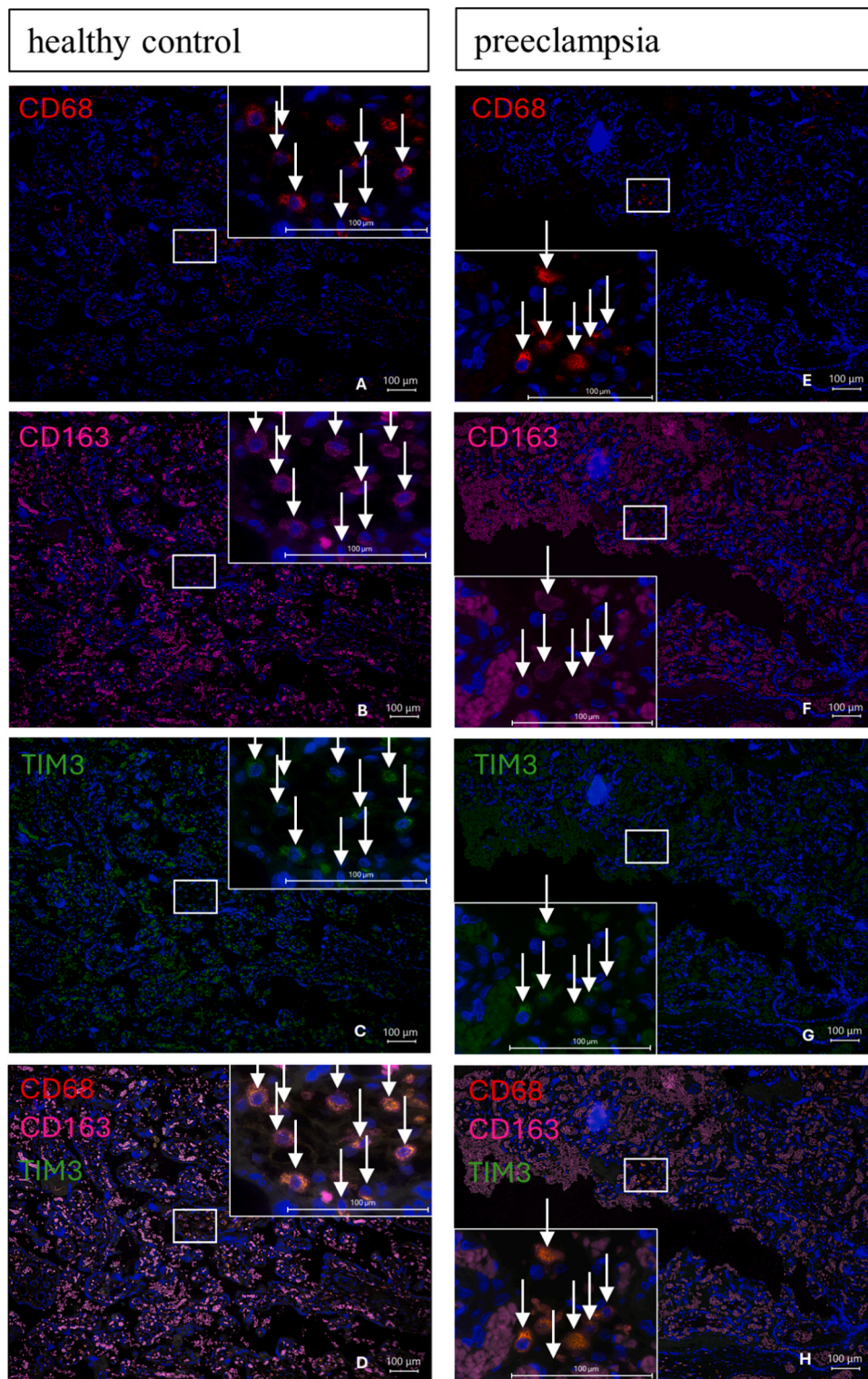
Fig. 3. Representative slides of triple immunofluorescence staining in the chorionic villi of a control placenta (A-D) and a preeclamptic placenta (E-H). Parts A and E show the immunofluorescence of CD68 (red), parts B and F the immunofluorescence of CD163 (pink) and parts C and G the immunofluorescence of TIM-3 (green). In the parts D and H all three markers are shown together in one picture. The arrows mark the HBCs which are TIM-3 positive in the triple staining. Pictures were taken with a 10x lens. The inserts represent a magnification with a 40x lens with additional zoom. The white frame shows where the magnified pictures are taken from. Scale bars are 100 μm.

3.5. Double immunofluorescence staining of TIM-3 with CD3, CD19 and CD56

Double immunofluorescence staining was performed for TIM-3 together with markers for other immune cells (CD3 for T cells, CD19 for B cells and CD56 for NK cells). This can be seen in Figs. 7, 8 and 9. The expression of these markers and their co-expression with TIM-3 was analyzed within the chorionic villi, because previous studies showed the
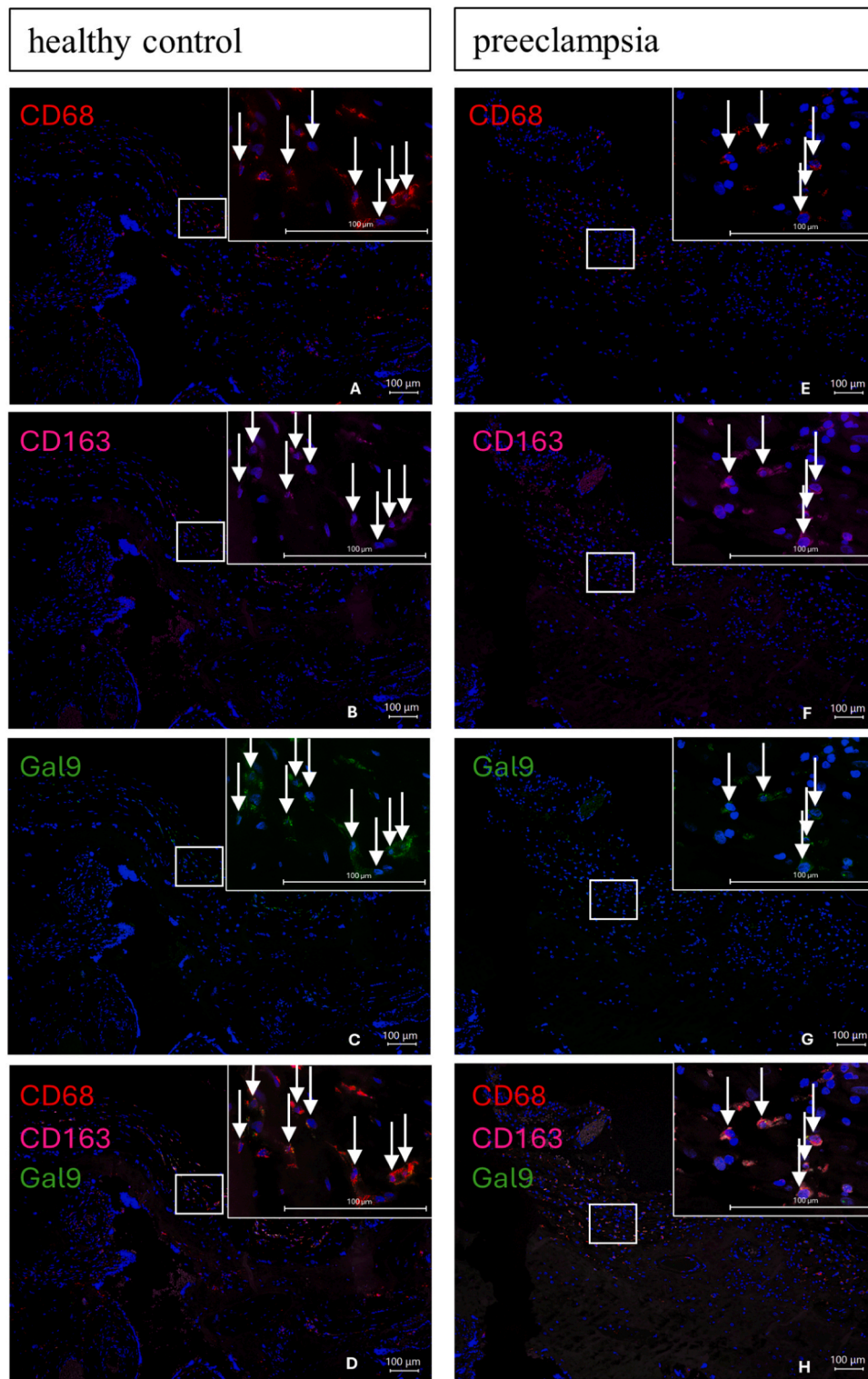
Fig. 4. Representative slides of triple immunofluorescence staining in the decidua of a control placenta (A-D) and a preeclamptic placenta (E-H). Parts A and E show the immunofluorescence of CD68 (red), parts B and F the immunofluorescence of CD163 (pink) and parts C and G the immunofluorescence of Gal-9 (green). In the parts D and H all three markers are shown together in one picture. The arrows mark the decidual macrophages which are Gal-9 positive in the triple staining. Pictures were taken with a 10x lens. The inserts represent a magnification with a 40x lens with additional zoom. The white frame shows where the magnified pictures are taken from. Scale bars are 100 μm.

existence of these immune cell populations within the chorionic villi (Toothaker et al., 2022).

For all three markers we only found very few cells within the villi (< 0,1 % of all cells). The B cells (CD19) and NK cells (CD56) showed a co-expression with TIM-3 while this was not seen in T cells (CD3). CD19-

positive cells were only found in the villi of the control placenta but not in the preeclamptic placenta.
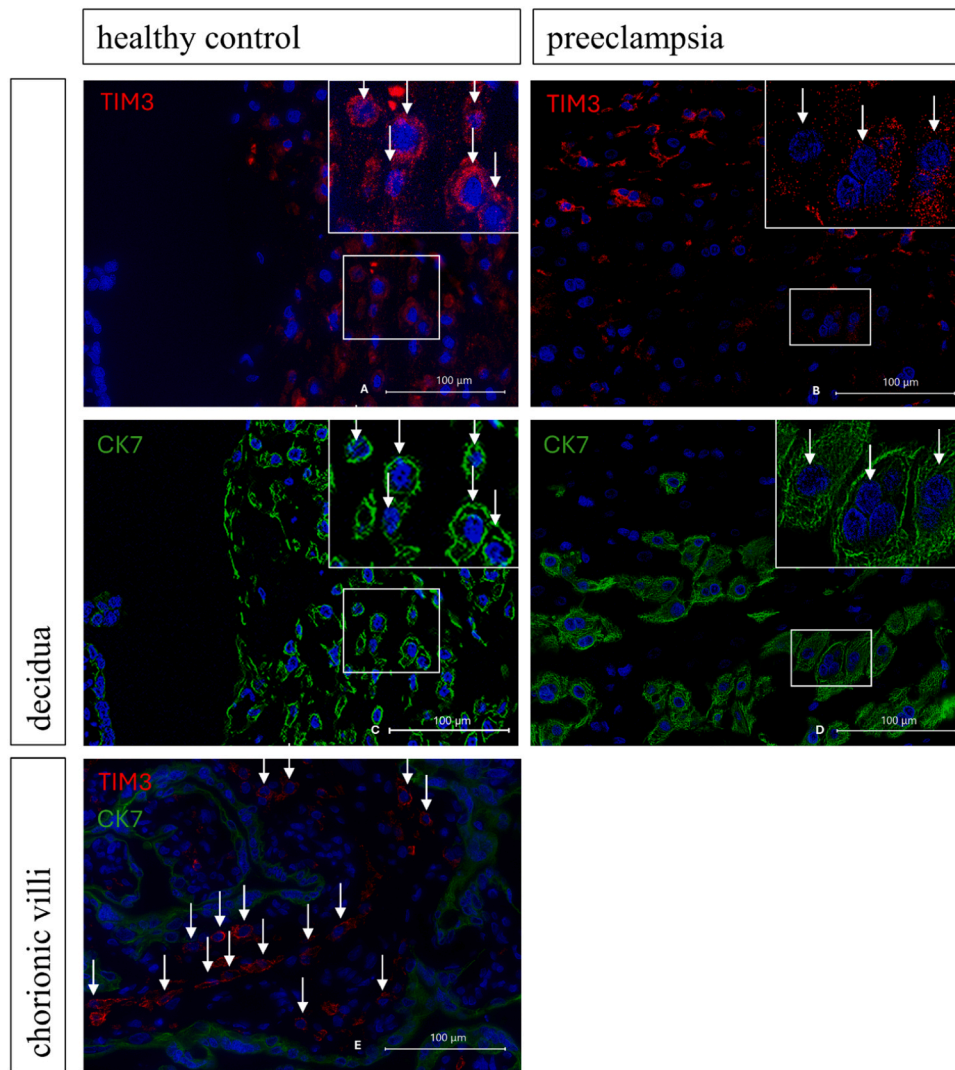
Fig. 5. Representative slides of double immunofluorescence staining in the decidua of a control placenta (A and C) and a preeclamptic placenta (B and D). Parts A and B show the immunofluorescence staining of TIM-3 (red), parts C and D the immunofluorescence staining of CK7 (green). The arrows mark the extravillious trophoblast cells which are TIM-3 positive. Part E shows the double staining within the chorionic villi of a control placenta. The arrows mark the TIM-3 positive Hofbauer cells. Pictures were taken with a 40x lens. The inserts represent a magnification with additional zoom. Scale bars are 100 μm.

4. Discussion

Preeclampsia is a pregnancy-specific disease with high fetal and maternal morbidity and mortality. As known so far, not only defective trophoblast invasion with impaired placentation, oxidative stress and endothelial dysfunction but also inflammation and modifications of immune reactions play an important role in the pathogenesis of the disease (Aggarwal et al., 2019; Harmon et al., 2016; Rambaldi et al., 2019; Rana et al., 2019; Vishnyakova et al., 2021; Yeh et al., 2013). This is a particularly difficult condition because it disrupts the adjusted and well matched immune responses which are crucial for upholding the tolerance of the fetus within the mother (Mor and Cardenas, 2010).

A disruption of one of the most important immune checkpoint systems, the TIM-3/Gal-9-system, can lead to proinflammation as mentioned above. Therefore, the goal of this study was to investigate its expression on macrophages within the placenta by immunohistochemistry and immunofluorescence staining.

The results characterizing the macrophage markers CD68 (pan-macrophage marker) and CD163 (M2-macrophage marker) within the same study cohort have already been published in our previous publication and were shown to be significantly downregulated in preeclamptic placentas just like the proteins PD1 and PD-L1 (Mittelberger et al., 2023).

Within this study we showed that the expression of TIM-3 on decidual macrophages did not differ between the two study groups. Distinguishing by fetal sex showed an upregulation of TIM-3 only in female offspring. An animal study previously performed by Wang et al., 2019 showed that the blockade of TIM-3 could lead to greater susceptibility for pregnancy loss by altering cytokine profiles of decidual T cells (Wang et al., 2019). This shows that TIM-3 is an important molecule at the feto-maternal-interface for maintaining pregnancy. Therefore, the upregulation of the TIM-3 receptor in female offspring found in the present study could protect female infants by inducing feto-maternal tolerance with lower susceptibility for pregnancy loss especially in early pregnancy. On the other hand, the study performed by Mao et al. showed an upregulation of TIM-3 and Gal-9 in decidual tissue of preeclamptic placentas which lead to an increased production of the proinflammatory cytokines INF-gamma and Interleukin-17 by Th1 and Th17 cells. This can lead to hyperimmune response (Hao et al., 2015). Following this, the upregulation of TIM-3 on maternal macrophages in preeclamptic cases with female offspring seen in our study could contribute to the mechanism mentioned there and to the
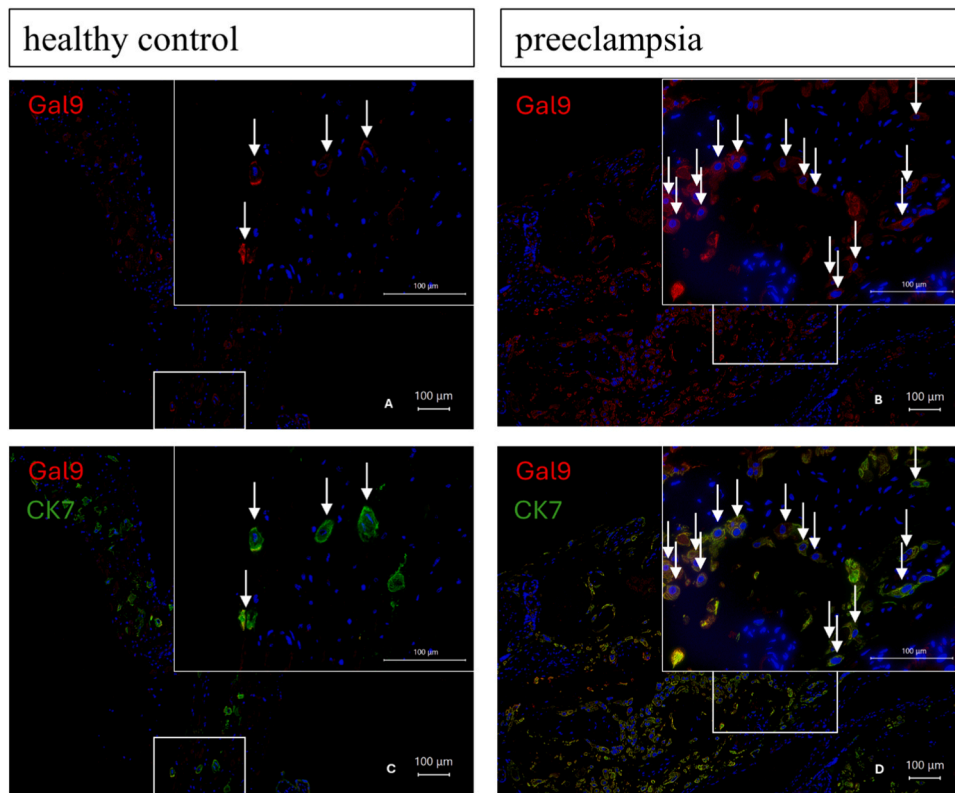
Fig. 6. Representative slides of double immunofluorescence staining in the decidua of a control placenta (A and C) and a preeclamptic placenta (B and D). Parts A and B show the immunofluorescence staining of Gal-9 (red), parts C and D the immunofluorescence staining of Gal-9 together with CK7 (green). The arrows mark the extravillious trophoblast cells which are Gal-9 positive. Pictures were taken with a 10x lens. The inserts represent a magnification with a 40x lens. Scale bars are 100 μm.

proinflammation seen in this pregnancy specific disease. This could make women carrying a female fetus more susceptible for developing preeclampsia.

The TIM-3 expression on Hofbauer cells, showed a significant downregulation in the preeclampsia group. This was evident in female and male offspring, which means there exists no sex specific difference. The activation of the TIM-3/Gal-9 pathway by Gal-9 binding to its receptor TIM-3 leads to a negative regulation of effector cells of the immune system such as T cells and thereby has an inhibitory effect on the immune system (Kandel et al., 2021). A downregulation of TIM-3 on Hofbauer cells could thereby lead to proinflammation within the chorionic villi because of the reduced binding capacity for Gal-9. As Hofbauer cells originate from yolk sac macrophages, which migrate to other organs through fetal development (Stremmel et al., 2018), this could also lead to inflammation and organ damage in later life of the infants.

We also investigated the co-expression of T cells, B cells and NK cells with TIM-3 within the chorionic villi by double immunofluorescence. Toothaker et al. already detected the existence of these cells within the chorionic villi by cyTOF and immunofluorescence (Toothaker et al., 2022). For all three markers we only found very few positive cells, so these other immune cells only make up a very small fraction of all cells within the chorionic villi (< 0,1 %). The majority of immune cells within the villi are macrophages. Although we found a co-expression of CD19 and CD56 with TIM-3 we believe that our quantitative analysis of TIM-3 and Gal-9 expression on macrophages and Hofbauer cells is not influenced by this small number of scattered other immune cells.

The protein Gal-9 was shown to be significantly downregulated on decidual macrophages and on Hofbauer cells in the preeclampsia group. This was only significant in male offspring but not in female offspring. The downregulation within the decidua could lead to local inflammation and thereby disrupt the feto-maternal tolerance which is important for

maintaining a healthy pregnancy. Within the Hofbauer cells the reduction of Gal-9 could again lead to proinflammation in other fetal organs by the migration of Hofbauer cells throughout fetal development and thereby to fetal programming. It is well known that male premature infants have a disadvantage in morbidity and mortality compared to female ones (Vu et al., 2018). Because this downregulation of Gal-9 in the preeclamptic placenta is only significant in male offspring it could contribute to the disadvantage of male premature and low birthweight infants. Whether there also exists a sex specific difference in morbidity and mortality in infants born after preeclampsia still needs further research. A study performed by Li et al. showed that the protein Gal-9 is an important key player in promoting tube formation during early placentation (Htr et al., 2021). A downregulation of the protein in preeclampsia could thereby contribute to the abnormal placenta, defective trophoblast invasion and the faulty spiral arteries seen in the pathogenesis of the disease.

The sex specific differences found here have already been shown within the PD1/PD-L1 system in our previous study by a downregulation of PD-L1 on maternal macrophages in preeclampsia with male offspring. The present study once more highlights the urgent need for further research regarding sex specific differences in preeclamptic offspring. It is well known that fetal sex influences the maternal immune system in different ways, for example by alterations in the cytokine profile. The sex-specific differences shown in our study could thereby contribute to alterations in the maternal immune system by causing proinflammation (Baines and West, 2023).

Our study suspects a downregulation of TIM-3 and an upregulation of Gal-9 in extravillious trophoblasts and syncytiotrophoblast cells in preeclampsia compared to healthy controls. This assumption can be made looking at the results of the immunohistochemical staining. The double immunofluorescense staining of TIM-3 with CK7 as a marker for
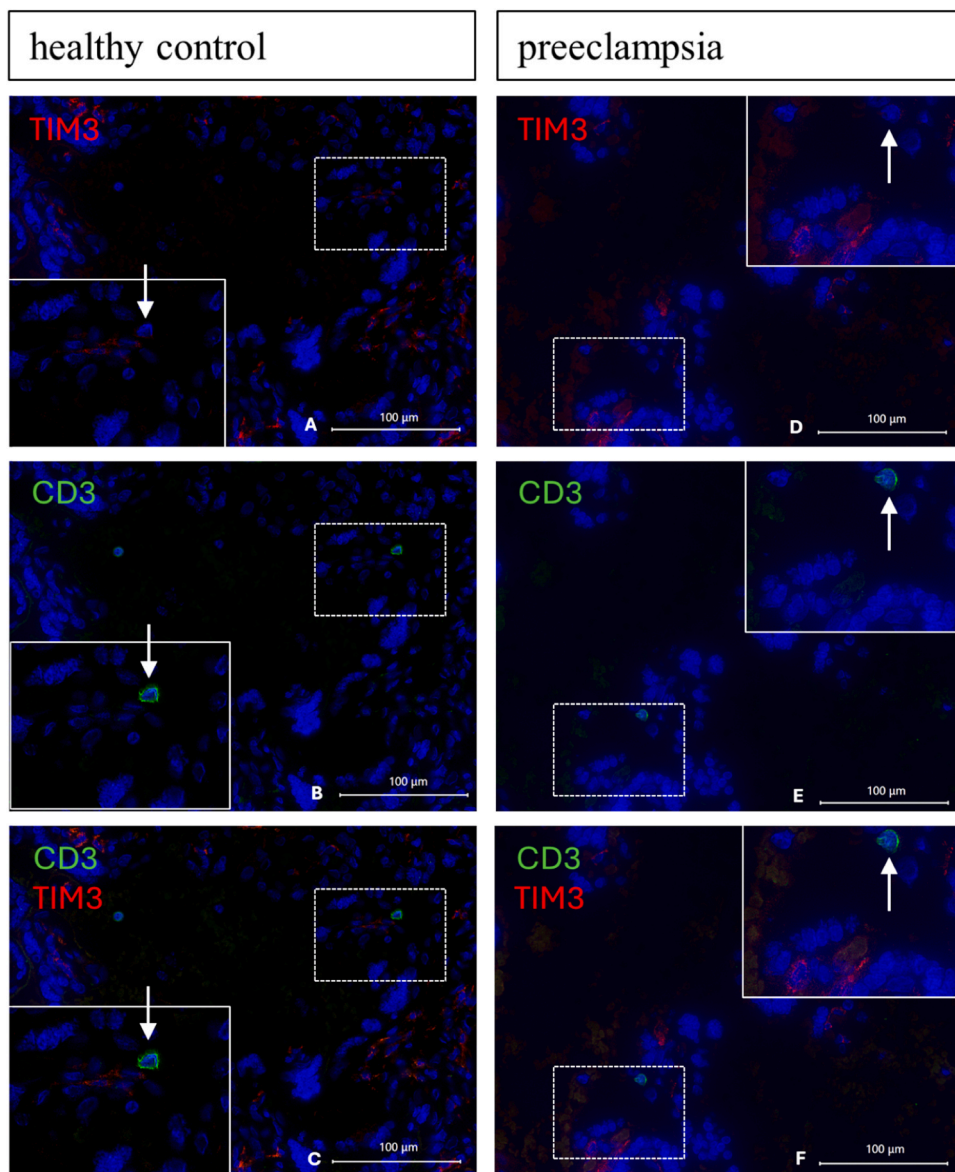
Fig. 7. Representative slides of double immunofluorescence staining in the chorionic villi of a control placenta (A-C) and a preeclamptic placenta (D-F). Parts A and D show the immunofluorescence staining of TIM-3 (red), parts B and E the immunofluorescence staining of CD3 (green) and parts C and F show TIM-3 together with CD3. The arrows mark the cells which are CD3 positive. No co-staining of the two markers can be seen. Pictures were taken with a 40x lens. The inserts represent a magnification with a 40x lens with additional zoom. Scale bars are 100 μm.
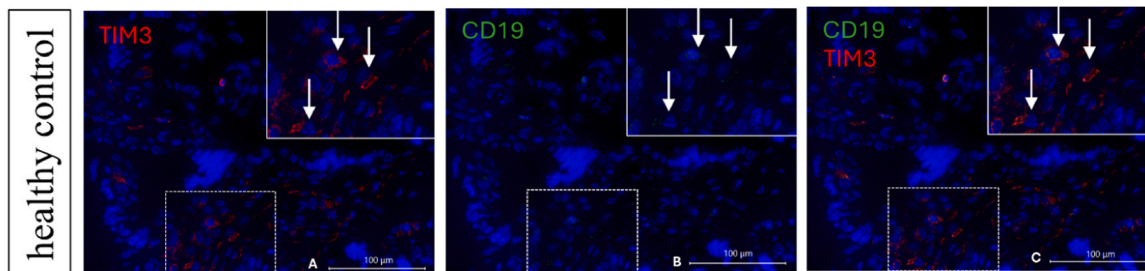

Fig. 8. Representative slides of double immunofluorescence staining in the chorionic villi of a control placenta. Part A shows the immunofluorescence staining of TIM-3 (red), part B the immunofluorescence staining of CD19 (green) and part C shows TIM-3 together with CD19. The arrows mark the cells which are CD19 positive. A co-staining of the two markers can be seen. Pictures were taken with a 40x lens. The inserts represent a magnification with a 40x lens with additional zoom. Scale bars are 100 μm.
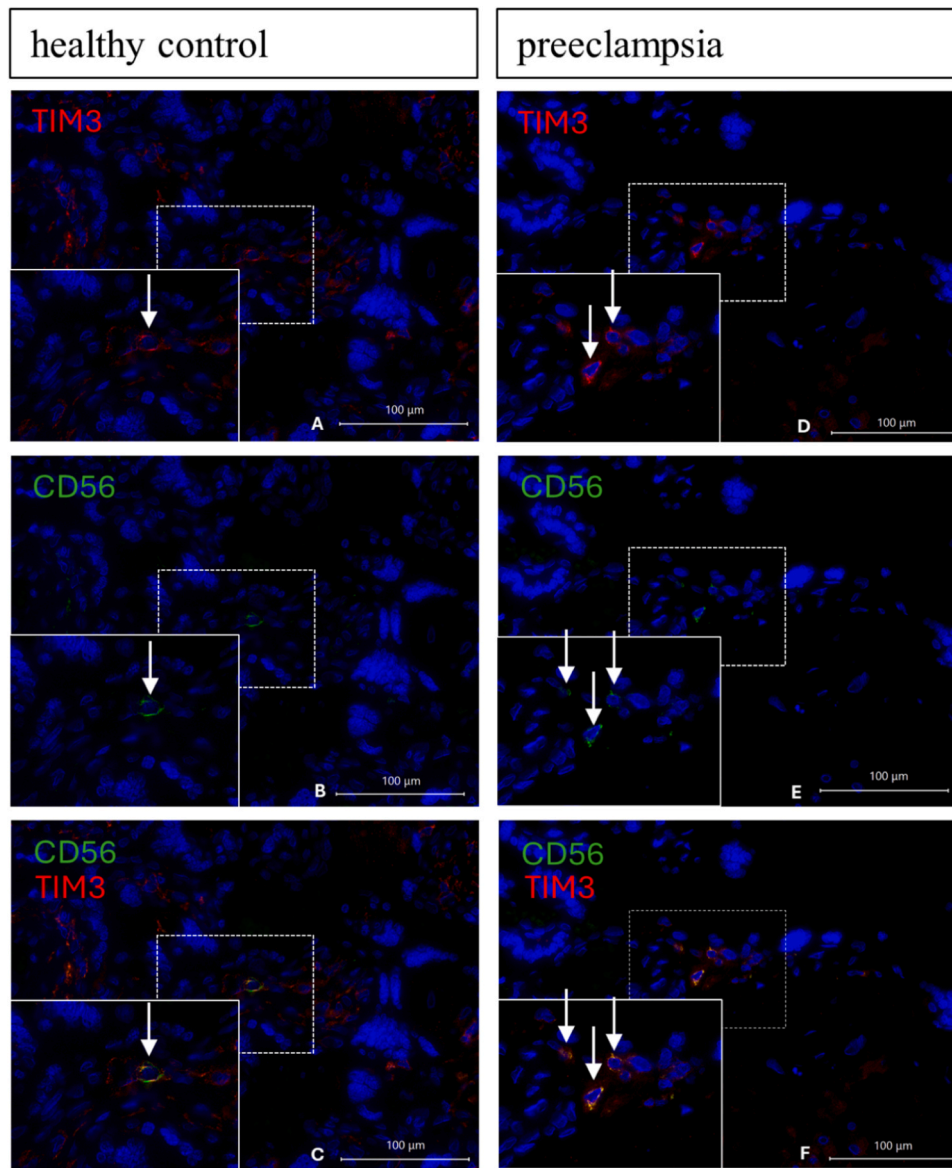
Fig. 9. Representative slides of double immunofluorescence staining in the chorionic villi of a control placenta (A-C) and a preeclamptic placenta (D-F). Parts A and D show the immunofluorescence staining of TIM-3 (red), parts B and E the immunofluorescence staining of CD56 (green) and parts C and F show TIM-3 together with CD56. The arrows mark the cells which are CD56 positive. A co-staining of the two markers can be seen Pictures were taken with a 40x lens. The inserts represent a magnification with a 40x lens with additional zoom. Scale bars are 100 μm.

extravillious trophoblast cells showed some cells with co-expression in the control and in the preeclampsia group. It was much weaker in the preeclamptic placenta, which can probably be explained by the down-regulation of TIM-3 within this group like already seen in the immunohistochemical staining. We found no co-expression of TIM-3 and CK7 within the Syncytiotrophoblast. The double staining of Gal-9 and CK7 clearly showed the suspected upregulation of Gal-9 on extravillious trophoblasts in the preeclamptic group. In order to closer examine the difference of immune checkpoint molecule expression on trophoblast cells further studies are needed using flow cytometry to sort trophoblast cells in fresh samples. Li et al. performed a study in 2021 showing that blockade of TIM-3 on extravillious trophoblasts resulted in their abnormal interaction with decidual immune cells and thereby leading to poor placental development (Li et al., 2021). The suspected differences in extravillious trophoblasts shown in our study could thereby point to an involvement of the immune checkpoint molecules in the development of preeclampsia but need further research. The expression of TIM-3 and Gal-9 on syncytiotrophoblasts has not yet been studied. Because

these cells play a crucial role in maintaining the placental barrier, alterations in immune checkpoint systems like the one we suspect in our study could disrupt this barrier by influencing the local immune system. Further studies are needed here.

In this patient cohort 14 out of the 40 preeclampsia cases simultaneously also had a HELLP-syndrome (hemolysis, elevated liver enzymes and low platelets) or fetal growth restriction (FGR) which often accompany preeclampsia. Whether these conditions confound the shown results cannot be answered within this analysis and must be investigated in further studies.

As a strength of this study, we see the breakdown of the data by fetal sex. A possible difference in morbidity and mortality depending on the sex of the offspring in preeclampsia cases needs further investigation.

In further studies the two study groups should be matched by clinical data such as BMI in order to rule out confounders and the number of counted image sections should be raised for more representative data. Fresh samples and flow cytometry could be used to sort different macrophages and trophoblast cells and closer examine the immune

checkpoint molecules directly on the sorted cells.

In conclusion, our study shows that the variations in the expression of TIM-3 and Gal-9 on placental macrophages might play an important role in the pathogenesis of preeclampsia by promoting pro-inflammation. This could be a new target in the therapy of preeclampsia in the future.

CRediT authorship contribution statement

Christian Dannecker: Supervision, Funding acquisition, Formal analysis, Data curation. **Udo Jeschke:** Writing – original draft, Supervision, Project administration, Methodology, Conceptualization. **Nina Ditsch:** Resources, Funding acquisition, Formal analysis, Data curation. **Fabian Garrido:** Visualization, Validation, Software. **Manuela Franitza:** Validation, Software, Resources, Funding acquisition, Formal analysis. **Marina Seefried:** Writing – review & editing, Resources, Data curation. **Johanna Mittelberger:** Writing – original draft, Investigation, Formal analysis, Data curation. **Christina Kuhn:** Visualization, Validation, Supervision, Resources, Methodology, Investigation. **Sanja Löb:** Software, Resources, Data curation, Conceptualization.

Declaration of Competing Interest

N.D. reports funding from MSD, Novartis, Pfizer, Roche, AstraZeneca, TEVA, Mentor, and MCI Healthcare. U.J. received travel money from pfm. C.D. is funded by Roche, AstraZeneca, TEVA, Mentor, and MCI Healthcare. All other authors declare no conflict of interest.

Appendix A. Supporting information

Supplementary data associated with this article can be found in the online version at doi:10.1016/j.jri.2024.104296.

References

Aggarwal, R., Jain, A.K., Mittal, P., Kohli, M., Jawanjal, P., Rath, G., 2019. Association of pro- and anti-inflammatory cytokines in preeclampsia. J. Clin. Lab. Anal. 33, 1–10. https://doi.org/10.1002/jcla.22834.
Ander, S.E., Diamond, M.S., Coyne, C.B., 2019. Immune responses at the maternal-fetal interface. Sci. Immunol. 4 https://doi.org/10.1126/sciimmunol.aat6114.
Baines, K.J., West, R.C., 2023. Sex differences in innate and adaptive immunity impact fetal, placental, and maternal health†. Biol. Reprod. 109, 256–270. https://doi.org/10.1093/biolre/ioad072.
Bürk, M.R., Troeger, C., Brinkhaus, R., Holzgreve, W., Hahn, S., 2001. Severely reduced presence of tissue macrophages in the basal plate of pre-eclamptic placentae. Placenta 22, 309–316. https://doi.org/10.1053/plac.2001.0624.
Hao, H., He, M., Li, J., Zhou, Y., Dang, J., Li, F., Yang, M., Deng, D., 2015. Upregulation of the Tim-3/Gal-9 pathway and correlation with the development of preeclampsia. Eur. J. Obstet. Gynecol. Reprod. Biol. 194, 85–91. https://doi.org/10.1016/j.ejogrb.2015.08.022.
Harmon, A.C., Cornelius, D.C., Amaral, L.M., Faulkner, J.L., Cunningham, M.W., Wallace, K., Lamarca, B., 2016. The role of inflammation in the pathology of preeclampsia Preeclampsia: hypertension During Pregnancy. Clin. Sci. 130, 409–419. 〈https://doi.org/10.1042/CS20150702.The〉.
Htr, G.-, Li, M., Peng, X., Qian, J., Sun, F., Chen, C., Wang, S., Zhang, J., Du, M., 2021. Galectin-9 regulates HTR8/SVneo function via JNK signaling 1626, 1–10.
Huang, S.J., Zenclussen, A.C., Chen, C.P., Basar, M., Yang, H., Arcuri, F., Li, M., Kocamaz, E., Buchwalder, L., Rahman, M., Kayisli, U., Schatz, F., Toti, P., Lockwood, C.J., 2010. The implication of aberrant GM-CSF expression in decidual cells in the pathogenesis of preeclampsia. Am. J. Pathol. 177, 2472–2482. https://doi.org/10.2353/ajpath.2010.091247.
Kandel, S., Adhikary, P., Li, G., Cheng, K., 2021. The TIM3/Gal9 signaling pathway: an emerging target for cancer immunotherapy. Cancer Lett. 510, 67–78. https://doi.org/10.1016/j.canlet.2021.04.011.
Li, M., Piao, L., Chen, C.P., Wu, X., Yeh, C.C., Masch, R., Chang, C.C., Huang, S.J., 2016. Modulation of decidual macrophage polarization by macrophage colony-stimulating factor derived from first-trimester decidual cells: implication in Preeclampsia. Am. J. Pathol. 186, 1258–1266. https://doi.org/10.1016/j.ajpath.2015.12.021.
Li, M., Sun, F., Qian, J., Chen, L., Li, D., Wang, S., Du, M., 2021. Tim-3/CTLA-4 pathways regulate decidual immune cells-extravillous trophoblasts interaction by IL-4 and IL-10. FASEB J. 35 https://doi.org/10.1096/fj.202100142R.
Mittelberger, J., Seefried, M., Franitza, M., Garrido, F., Ditsch, N., Jeschke, U., Dannecker, C., 2022. The role of the immune checkpoint molecules PD-1/PD-L1 and TIM-3/Gal-9 in the pathogenesis of preeclampsia— a narrative review. Med 58, 1–12. https://doi.org/10.3390/medicina58020157.
Mittelberger, J., Seefried, M., Löb, S., Kuhn, C., Franitza, M., Garrido, F., Wild, C.M., Ditsch, N., Jeschke, U., Dannecker, C., 2023. The programmed cell death protein 1 (PD1) and the programmed cell death ligand 1 (PD-L1) are significantly downregulated on macrophages and Hofbauer cells in the placenta of preeclampsia patients. J. Reprod. Immunol. 157 https://doi.org/10.1016/j.jri.2023.103949.
Mohamed Khosroshahi, L., Parhizkar, F., Kachalaki, S., Aghebati-Maleki, A., Aghebati-Maleki, L., 2021. Immune checkpoints and reproductive immunology: pioneers in the future therapy of infertility related Disorders? Int. Immunopharmacol. 99, 107935 https://doi.org/10.1016/j.intimp.2021.107935.
Mor, G., Cardenas, I., 2010. The immune system in pregnancy: a unique complexity. Am. J. Reprod. Immunol. 63, 425–433. https://doi.org/10.1111/j.1600-0897.2010.00836.x.
Rambaldi, M.P., Weiner, E., Mecacci, F., Bar, J., Petraglia, F., 2019. Immunomodulation and preeclampsia. Best. Pract. Res. Clin. Obstet. Gynaecol. 60, 87–96. https://doi.org/10.1016/j.bpobgyn.2019.06.005.
Rana, S., Lemoine, E., Granger, J., Karumanchi, S.A., 2019. Preeclampsia: pathophysiology, challenges, and perspectives. Circ. Res. 124, 1094–1112. https://doi.org/10.1161/CIRCRESAHA.118.313276.
Reister, F., Frank, H.G., Kingdom, J.C.P., Heyl, W., Kaufmann, P., Rath, W., Huppertz, B., 2001. Macrophage-induced apoptosis limits endovascular trophoblast invasion in the uterine wall of preeclamptic women. Lab. Investig. 81, 1143–1152. https://doi.org/10.1038/labinvest.3780326.
Reyes, L., Golos, T.G., 2018. Hofbauer cells: their role in healthy and complicated pregnancy. Front. Immunol. 9, 1–8. https://doi.org/10.3389/fimmu.2018.02628.
Stremmel, C., Schuchert, R., Wagner, F., Thaler, R., Weinberger, T., Pick, R., Mass, E., Ishikawa-Ankerhold, H.C., Margraf, A., Hutter, S., Vagnozzi, R., Klapproth, S., Frampton, J., Yona, S., Scheiermann, C., Molkentin, J.D., Jeschke, U., Moser, M., Sperandio, M., Massberg, S., Geissmann, F., Schulz, C., 2018. Yolk sac macrophage progenitors traffic to the embryo during defined stages of development. Nat. Commun. 9 https://doi.org/10.1038/s41467-017-02492-2.
Sukmanee, J., Liabsuetrakul, T., 2022. Risk of future cardiovascular diseases in different years postpartum after hypertensive disorders of pregnancy: a systematic review and meta-analysis. Med. (Baltim.) 101, e29646. https://doi.org/10.1097/MD.0000000000029646.
Tang, Z., Buhimschi, I.A., Buhimschi, C.S., Tadesse, S., Norwitz, E., Niven-Fairchild, T., Huang, S.T.J., Guller, S., 2013. Decreased levels of folate receptor-β and reduced numbers of fetal macrophages (hofbauer cells) in placentas from pregnancies with severe pre-eclampsia. Am. J. Reprod. Immunol. 70, 104–115. https://doi.org/10.1111/aji.12112.
Toothaker, J.M., Olaloye, O., McCourt, B.T., McCourt, C.C., Silva, T.N., Case, R.M., Liu, P., Yimlamai, D., Tseng, G., Konnikova, L., 2022. Immune landscape of human placental villi using single-cell analysis. Dev 149. https://doi.org/10.1242/dev.200013.
Tranquilli, A.L., Brown, M.A., Zeeman, G.G., Dekker, G., Sibai, B.M., 2013. The definition of severe and early-onset preeclampsia. Statements from the International Society for the Study of Hypertension in Pregnancy (ISSHP). Pregnancy Hypertens. 3, 44–47. https://doi.org/10.1016/j.preghy.2012.11.001.
Valensise, H., Vasapollo, B., Gagliardi, G., Novelli, G.P., 2008. Early and Late preeclampsia: two different maternal hemodynamic states in the latent phase of the disease. Hypertension 52, 873–880. https://doi.org/10.1161/HYPERTENSIONAHA.108.117358.
Vest, A.R., Cho, L.S., 2012. Hypertension in pregnancy. Cardiol. Clin. 30, 407–423. https://doi.org/10.1016/j.ccl.2012.04.005.
Vishnyakova, P., Poltavets, A., Nikitina, M., Muminova, K., Potapova, A., Vtorushina, V., Loginova, N., Midiber, K., Mikhaleva, L., Lokhonina, A., Khodzhaeva, Z., Pyregov, A., Elchaninov, A., Fatkhudinov, T., Sukhikh, G., 2021. Preeclampsia: inflammatory signature of decidual cells in early manifestation of disease. Placenta 104, 277–283. https://doi.org/10.1016/j.placenta.2021.01.011.
Vu, H.D., Dickinson, C., Kandasamy, Y., 2018. Sex difference in mortality for premature and low birth weight neonates: a systematic review. Am. J. Perinatol. 35, 707–715. https://doi.org/10.1055/s-0037-1608876.
Wang, S., Chen, C., Li, M., Qian, J., Sun, F., Li, Y., Yu, M., Wang, M., Zang, X., Zhu, R., Li, D., Du, M., 2019. Blockade of CTLA-4 and Tim-3 pathways induces fetal loss with altered cytokine profiles by decidual CD4 + T cells. Cell Death Dis. 10 https://doi.org/10.1038/s41419-018-1251-0.
Williams, P.J., Bulmer, J.N., Searle, R.F., Innes, B.A., Robson, S.C., 2009. Altered decidual leucocyte populations in the placental bed in pre-eclampsia and foetal growth restriction: a comparison with late normal pregnancy. Reproduction 138, 177–184. https://doi.org/10.1530/REP-09-0007.
Xu, J., Li, T., Wang, Y., Xue, L., Miao, Z., Long, W., Xie, K., 2022. The Association Between Hypertensive Disorders in Pregnancy and the Risk of Developing Chronic Hypertension 9, 1–15. https://doi.org/10.3389/fcvm.2022.897771.
Yang, S.W., Cho, E.H., Choi, S.Y., Lee, Y.K., Park, J.H., Kim, M.K., Park, J.Y., Choi, H.J., Lee, J.I., Ko, H.M., Park, S.H., Hwang, H.S., Kang, Y.S., 2017. DC-SIGN expression in Hofbauer cells may play an important role in immune tolerance in fetal chorionic villi during the development of preeclampsia. J. Reprod. Immunol. 124, 30–37. https://doi.org/10.1016/j.jri.2017.09.012.
Yao, Y., Xu, X.H., Jin, L., 2019. Macrophage polarization in physiological and pathological pregnancy. Front. Immunol. 10, 1–13. https://doi.org/10.3389/fimmu.2019.00792.
Yeh, C.C., Chao, K.C., Huang, S.J., 2013. Innate immunity, decidual cells, and preeclampsia. Reprod. Sci. 20, 339–353. https://doi.org/10.1177/1933719112450330.